Magnetic anisotropy in Fe/Cu(001) overlayers and interlayers: The high-moment ferromagnetic phase

B. Újfalussy
Institut für Technische Elektrochemie, Technische Universität Wien, Getreidemarkt 9/158, A-1060, Wien, Austria and Research Institute for Solid State Physics, Hungarian Academy of Sciences, H-1525 Budapest, P.O. Box 49, Hungary

L. Szunyogh
Institute of Physics, Technical University of Budapest, Budafoki út 8, H-1521, Budapest, Hungary and Institut für Technische Elektrochemie, Technische Universität Wien, Getreidemarkt 9/158, A-1060, Wien, Austria

P. Weinberger
Institut für Technische Elektrochemie, Technische Universität Wien, Getreidemarkt 9/158, A-1060, Wien, Austria
(Received 28 February 1996)

An extensive study of the magnetic anisotropy energies (MAE's) of the high-moment ferromagnetic phase of fcc Fe/Cu(001) overlayers and interlayers is presented in terms of the fully relativistic spin-polarized screened Korringa-Kohn-Rostoker method. Independent of the film thickness for free surfaces the orientation of the magnetization is found to be in-plane, while for capped films a perpendicular magnetization is predicted up to a switching thickness of five Fe monolayers. Based on an analysis of layer-resolved anisotropy energies it is shown that the main contribution to the MAE's arises from the Fe layer at the Fe/Cu interfaces. Particular features of the MAE's with respect to the number of cap layers as well as to the film thickness can be viewed in terms of an interfacial hybridization between Fe and Cu. By using the coherent-potential approximation the interdiffusion between the substrate and the magnetic film is shown to reduce the MAE dramatically. [S0163-1829(96)03638-7]

I. INTRODUCTION

The Fe/Cu(001) system is one of the most extensively studied magnetic thin film materials. Its structural and magnetic properties have always been expected to be rich. Due to the small epitaxial misfit, a good layer-by-layer growth of Fe on Cu(001) has been expected and also found experimentally, stabilizing the film in a structure related to the fcc phase of bulk Fe which is otherwise unstable at low temperatures. The measured heat of intermixing and surface tension indicates a tendency for surface segregation.[1,2] Furthermore, the balance of surface and interface free energies prefers the formation of a sandwiched structure (Cu/Fe/Cu).[1] It has been shown by several authors[3–9] that fcc iron films exhibit a rich magnetic structure, depending very sensitively on the atomic volume. In particular in Fe films grown on Cu(001) one distinguishes a high-moment ferromagnetic, a low-moment ferromagnetic, and a low-moment antiferromagnetic phase. At the lattice constant of Cu, the system is at the edge of all these phases; therefore small differences of strain can stabilize either one. Because of this peculiarity, it is difficult to trace compatible experimental data. Although there are some indications, both experimental[10–12] and theoretical,[13,14] that the ground state is antiferromagnetically ordered, the current — sometimes controversial — experimental situation makes it necessary to study each possible phase theoretically. In this paper we examine the magnetic anisotropy of the high-moment ferromagnetic phase, while the low-moment antiferromagnetic phase will be investigated elsewhere.

Presently there are two different types of experimental studies available. One kind of approach investigates Fe layer precipitates in a Cu matrix or periodic Fe/Cu multilayered systems.[15,16] The theoretical calculations of Guo *et al.*[18,19] can be related to these experimental efforts. The other type of experimental studies exploits thin-film epitaxy by growing atomic layers.[2–4,6,7] The recently developed screened Korringa-Kohn-Rostoker (SKKR) method[20,21] allows an exact theoretical treatment of both geometrical setups, namely, also the case of Fe overlayers on a semi-infinite Cu substrate. Furthermore, its extension to fully relativistic spin-polarized scattering[22] allows one to treat relativity and spin polarization simultaneously on the same theoretical level.

II. METHOD OF COMPUTATIONS

The spin-polarized relativistic screened Korringa-Kohn-Rostoker method as described in Ref. 22 has been employed in the present paper to calculate the electronic structure as well as the perpendicular magnetic anisotropy energies (MAE's) of the ferromagnetic multilayer systems $Cu_mFe_n/Cu(001)$ for $m=0$, 1, 2, and ∞ and $n=1,\ldots,6$. Here $m=\infty$ denotes the case of an Fe_n multilayer stacked into bulk Cu along the (001) direction. In the present study no layer relaxation effects were taken into account; i.e., the parent lattice corresponds to a fcc lattice with the lattice parameter of bulk copper (6.831 a.u.).

First, self-consistent calculations within the local spin density approximation (LSDA)[23] and the atomic sphere approximation (ASA) were carried out with the magnetic field pointing in each layer uniformly perpendicular to the surface (interface). At the vacuum/metal interface two monolayers of empty sphere potentials and at the Cu substrate/Fe film in-

TABLE I. Calculated local valence charges [electrons] of Fe atoms in $Cu_mFe_n/Cu(001)$ multilayers ($m=0,1,2,\infty$; $n=1,2,\ldots,6$). The numbering of Fe layers increases from the vacuum (or capped) side towards the bulk.

n	m	Fe(6)	Fe(5)	Fe(4)	Fe(3)	Fe(2)	Fe(1)
1	0						7.574
	1						7.852
	2						7.850
	∞						7.889
2	0					7.928	7.652
	1					7.923	7.925
	2					7.926	7.923
	∞					7.962	7.962
3	0				7.923	8.003	7.653
	1				7.927	7.997	7.926
	2				7.926	8.000	7.923
	∞				7.939	8.043	7.939
4	0			7.926	7.998	8.003	7.654
	1			7.926	8.001	7.998	7.925
	2			7.926	8.001	8.001	7.922
	∞			7.942	8.020	8.020	7.942
5	0		7.926	8.000	7.998	8.003	7.652
	1		7.926	8.000	8.002	7.998	7.925
	2		7.925	8.000	8.001	8.001	7.922
	∞		7.942	8.024	7.994	8.024	7.942
6	0	7.926	8.000	8.001	7.998	8.004	7.652
	1	7.925	8.000	8.000	8.001	7.998	7.925
	2	7.925	8.000	8.001	8.001	8.001	7.922
	∞	7.941	8.022	7.998	7.998	8.022	7.941

TABLE II. Calculated spin-only magnetic moments [μ_B] of Fe atoms in $Cu_mFe_n/Cu(001)$ multilayers ($m=0,1,2,\infty$; $n=1,2,\ldots,6$). The numbering of Fe layers increases from the vacuum (or capped) side towards the bulk.

n	m	Fe(6)	Fe(5)	Fe(4)	Fe(3)	Fe(2)	Fe(1)
1	0						2.784
	1						2.605
	2						2.579
	∞						2.537
2	0					2.585	2.794
	1					2.577	2.587
	2					2.558	2.593
	∞					2.536	2.536
3	0				2.557	2.489	2.820
	1				2.552	2.464	2.569
	2				2.558	2.461	2.593
	∞				2.544	2.418	2.544
4	0			2.536	2.382	2.470	2.826
	1			2.539	2.369	2.363	2.544
	2			2.548	2.403	2.414	2.588
	∞			2.536	2.383	2.383	2.536
5	0		2.554	2.429	2.392	2.490	2.843
	1		2.563	2.438	2.386	2.400	2.561
	2		2.557	2.421	2.401	2.436	2.599
	∞		2.544	2.386	2.402	2.386	2.544
6	0	2.559	2.448	2.412	2.419	2.503	2.845
	1	2.562	2.453	2.420	2.406	2.412	2.560
	2	2.559	2.426	2.410	2.412	2.439	2.600
	∞	2.549	2.411	2.415	2.415	2.411	2.549

terface at least two monolayers of Cu potentials were treated self-consistently. Energy integrations were performed along a semicircular contour using a 16-point Gaussian sampling on an asymmetric mesh. For the Brillouin zone integrations 45 $\mathbf{k}_\parallel$ points in the irreducible ($\frac{1}{8}$) wedge of the surface Brillouin zone (IBZ) have been used.

Second, the MAE's were determined within the force theorem. It should be noted that by using the force theorem the MAE is reduced to a sum of two contributions, namely, the band energy and the magnetostatic dipole-dipole interaction energy ΔE_b and ΔE_{dd}, respectively.[22] Here we use the notation $\Delta E_\alpha = E_\alpha^\parallel - E_\alpha^\perp$ ($\alpha = b$ or dd), where $\parallel$ and $\perp$ refer to the cases that in each layer the magnetic field points uniformly parallel or perpendicular to the surface (interface). When calculating ΔE_b, 325 $\mathbf{k}_\parallel$ points in the IBZ were found to ensure a relative accuracy of less than 5%. The magnetostatic dipole-dipole energy was calculated as described in the Appendix of Ref. 22.

III. RESULTS AND DISCUSSION

A. Electronic and magnetic structure

For the uncovered multilayers (see rows labeled by $m=0$ in Table I) a remarkable charge depletion characterizes the surface Fe layer [denoted be Fe(1)] and, though smaller, also the Fe layer closest to the substrate [Fe(n) for $n \geq 2$]. For thicker multilayers ($n \geq 3$) buried Fe layers [Fe(2), ... ,Fe($n-1$)] are nearly neutral. This asymmetry becomes fairly balanced when putting an additional Cu layer onto the Fe multilayer ($m=1$), whereby the charge distribution does not change significantly when depositing further Cu layers ($m=2$ and ∞). For $m=0$ the spin-only magnetic moments (see Table II) of Fe(1) are clearly enhanced as compared to buried Fe layers. Such an enhancement is a general property of ferromagnetic surfaces and can simply be attributed to band narrowing at the surface and to an enhanced electrostatic surface potential.[17] An increasing number of capping Cu layers rapidly forces the magnetic moment distribution of the multilayer system to become symmetric. Inspecting Table III one can see that the layer-resolved orbital moments systematically increase up to $n=4$ while for thicker Fe multilayers they start to decrease.

The present results for the symmetric interlayers ($m=\infty$) can be compared to those of Guo *et al.*,[18,19] who performed similar calculations for Fe_n/Cu_m multilayers ($n=1$, 3, and 5) by using the spin-polarized relativistic linear muffin-tin orbital (LMTO) technique with supercell geometry. As far as local quantities are concerned, very good agreement between the two types of approaches is found (see Table IV). Since, as we have checked, the different exchange-correlation functionals used in the two calculations — in the present work the functional of Vosko, Wilk, and Nusair,[23] while in Refs. 18 and 19 that of von Barth and Hedin[24] has been employed — can account only for minor differences, the occurring differences seen in Table IV have

TABLE III. Calculated orbital magnetic moments [μ_B] of Fe atoms in Cu_mFe_n/Cu(001) multilayers ($m=0,1,2,\infty$; $n=1,2,\ldots,6$). The numbering of Fe layers increases from the vacuum (or capped) side towards the bulk.

n	m	Fe(6)	Fe(5)	Fe(4)	Fe(3)	Fe(2)	Fe(1)
1	0						0.080
	1						0.074
	2						0.064
	∞						0.067
2	0					0.076	0.084
	1					0.079	0.082
	2					0.072	0.071
	∞					0.074	0.074
3	0				0.079	0.085	0.079
	1				0.074	0.086	0.085
	2				0.079	0.089	0.075
	∞				0.080	0.090	0.080
4	0			0.084	0.094	0.092	0.081
	1			0.084	0.088	0.092	0.089
	2			0.084	0.097	0.098	0.082
	∞			0.084	0.095	0.095	0.084
5	0		0.079	0.089	0.082	0.082	0.076
	1		0.077	0.085	0.075	0.083	0.085
	2		0.077	0.084	0.081	0.085	0.073
	∞		0.077	0.081	0.078	0.081	0.077
6	0	0.076	0.082	0.075	0.074	0.077	0.077
	1	0.074	0.076	0.070	0.066	0.074	0.080
	2	0.076	0.079	0.073	0.073	0.080	0.073
	∞	0.076	0.080	0.073	0.073	0.080	0.076

to be attributed either to supercell effects or to the energy linearization inherent to the LMTO method.

B. Magnetic anisotropy energies

In Fig. 1 the MAE's are displayed as a function of the Fe multilayer thickness for the free surface ($m=0$), with a cap of one Cu monolayer ($m=1$), and for the symmetric interlayers ($m=\infty$). Similar to the Fe_n/Au(001) system[22] ΔE_b is always positive (see Sec. II); i.e., it favors a perpendicular orientation for the magnetization. For the uncovered systems, however, it is too small to compensate the negative contribution of the magnetostatic dipole-dipole interaction to the MAE (ΔE_{dd}) and, therefore, our calculations predict an in-plane magnetization for any thickness of the Fe multilayer. It should be mentioned that this result obviously contradicts that of Lorenz and Hafner[25] who by using a recursion technique combined with the tight-binding LMTO method predicted a perpendicular magnetization for Fe_1/Cu(001) with a rather large ($\sim$ 2 meV) anisotropy energy.

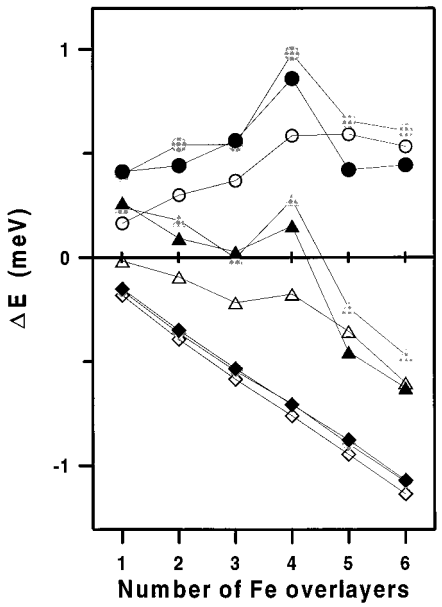

FIG. 1. Calculated magnetic anisotropy energies of Cu_mFe_n/Cu(001) multilayers for $m=0$ (open symbols), $m=1$ (shaded symbols), and $m=\infty$ (solid symbols). ΔE_b, circles; ΔE_{dd}, squares; $\Delta E=\Delta E_b+\Delta E_{\mathrm{dd}}$, triangles. Solid lines serve as a guide for the eye.

When the surface is covered by one or more Cu monolayers ($m\geqslant 1$) the situation becomes qualitatively different. As compared to the uncovered case, ΔE_b is considerably enhanced for $n\leqslant 4$, while for thicker Fe multilayers and for more than one capping Cu layer — as an example only the case of $m=\infty$ is shown in Fig. 1 — it is somewhat reduced. Generally, the largest MAE can be found for the case of one covering Cu layer. As mentioned before, a systematic maximum of the layer-resolved orbital moments was found for $n=4$. Since in terms of second-order perturbation theory the orbital moments are correlated with the MAE (see, e.g., Refs. 26 and 27), a similar behavior of the calculated ΔE_b's is expected. For the capped systems, this clearly shows up as a corresponding peak in ΔE_b at $n=4$. Inspecting the total MAE curves in Fig. 1 it is apparent that for multilayers capped by Cu a reorientation from perpendicular to an in-plane magnetization would occur without this anomalous peak at $n=3$, whereas in fact it occurs at $n=5$.

Table V summarizes the calculated anisotropies of the orbital moments and band energies for the Fe_n interlayers ($n=1$, 3, and 5) in comparison to those of Refs. 18 and 19. Both the magnitude of the calculated MAE's and their trend with the multilayer thickness are very similar in these two different calculations. In fact it is not surprising that the best agreement is found for the monolayer system, because in the series of the Fe_1Cu_5, Fe_3Cu_3, and Fe_5Cu_3 repeated se-

TABLE IV. Local valence charges (Q_{val}), spin-only magnetic moments (m_{spin}), and orbital moments (m_{orb}) for Fe_n interlayers ($n=1$, 3, and 5) in Cu(001). Respective first columns refer to the present calculations, second columns to the results of Guo *et al.* (Refs. 18,19). Since the corresponding multilayer systems are symmetric, only the first $(n+1)/2$ Fe layers are listed.

n		Q_{val} [electrons]		m_{spin} [μ_B]		m_{orb} [μ_B]	
1	Fe(1)	7.889	7.894	2.537	2.435	0.067	0.068
3	Fe(1)	7.939	7.939	2.544	2.505	0.080	0.083
	Fe(2)	8.043	8.044	2.418	2.353	0.090	0.092
5	Fe(1)	7.942	7.940	2.544	2.517	0.077	0.082
	Fe(2)	8.024	8.022	2.386	2.339	0.081	0.085
	Fe(3)	7.994	7.998	2.402	2.323	0.078	0.077

TABLE V. Total orbital moment anisotropies ($\Delta m_{\rm orb}=m^{\parallel}_{\rm orb}-m^{\perp}_{\rm orb}$) and band energy anisotropies ($\Delta E_b=E_b^{\parallel}-E_b^{\perp}$) for Fe_n interlayers ($n=1$, 3, and 5) in Cu(001). Respective first columns refer to the present calculations, second columns to the results of Guo *et al.* (Refs. 18,19). Since the corresponding multilayer systems are symmetric, only the first $(n+1)/2$ Fe layers are listed.

n	$\Delta m_{\rm orb}$ [μ_B]		ΔE_b [meV]	
1	-0.015	-0.013	0.412	0.428
3	-0.031	-0.043	0.562	0.665
5	-0.048	-0.028	0.422	0.597

quences used in Refs. 18 and 19 the first one is expected to have the smallest supercell effects on Fe.

C. Layer- and spin-resolved analysis of the MAE

In the case of Fe_n/Au(001) multilayers[22] an analysis of ΔE_b in terms of layer-resolved contributions has been proved to be very useful. For $m=0$, 1, and ∞ the layer-resolved contributions of ΔE_b are displayed in Figs. 2, 3, and 4, respectively. In addition, by using a transformation from the relativistic (κ,μ) angular momentum basis to the nonrelativistic (ℓ,m,σ) basis[28,29] (see also Ref. 30), it is possible to partition ΔE_b at least qualitatively into a majority ($\sigma=\frac{1}{2}$) and a minority ($\sigma=-\frac{1}{2}$) contribution, $\Delta E_b^{\uparrow}$ and $\Delta E_b^{\downarrow}$, respectively. It should be noted that this kind of classification is in principle incorrect within a fully relativistic treatment, because the spin eigenvalue σ is not a good quantum number in the presence of spin-orbit coupling. For strong ferromagnets like iron, however, a nonrelativistic description provides a more familiar visualization. The above-mentioned transformation enables also a qualitative interpretation of the present results in terms of a perturbative approach based on the (semirelativistic) Pauli-Schrödinger equation.[26,27]

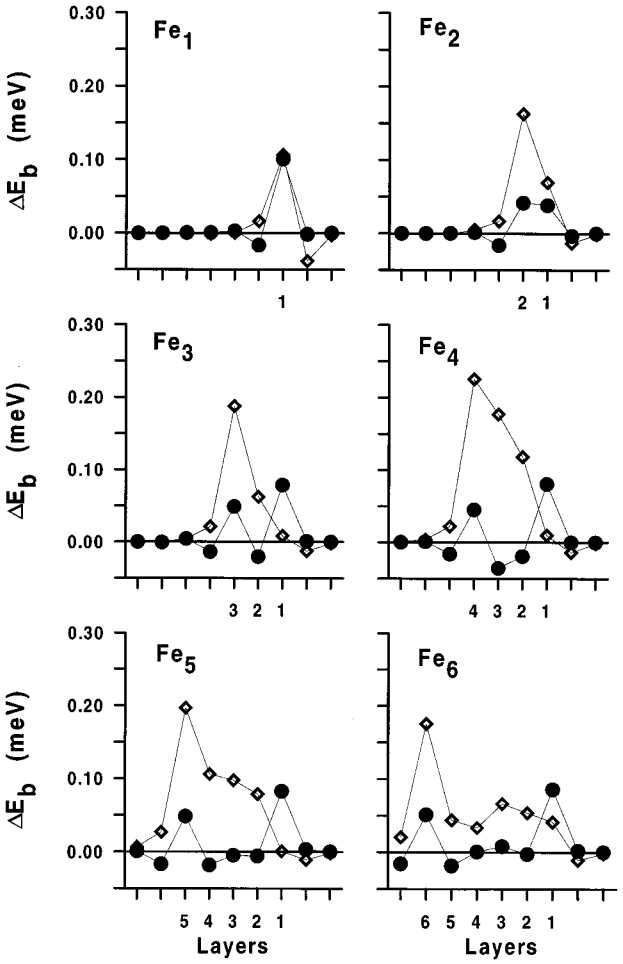

FIG. 2. Layer-resolved band energy contributions to the MAE for Fe_n/Cu(001) multilayers. Starting from the surface, only the Fe layers are numbered. The contributions related to the minority and majority channels (see text) are shown as open squares and solid circles, respectively. Solid lines serve as a guide for the eye.

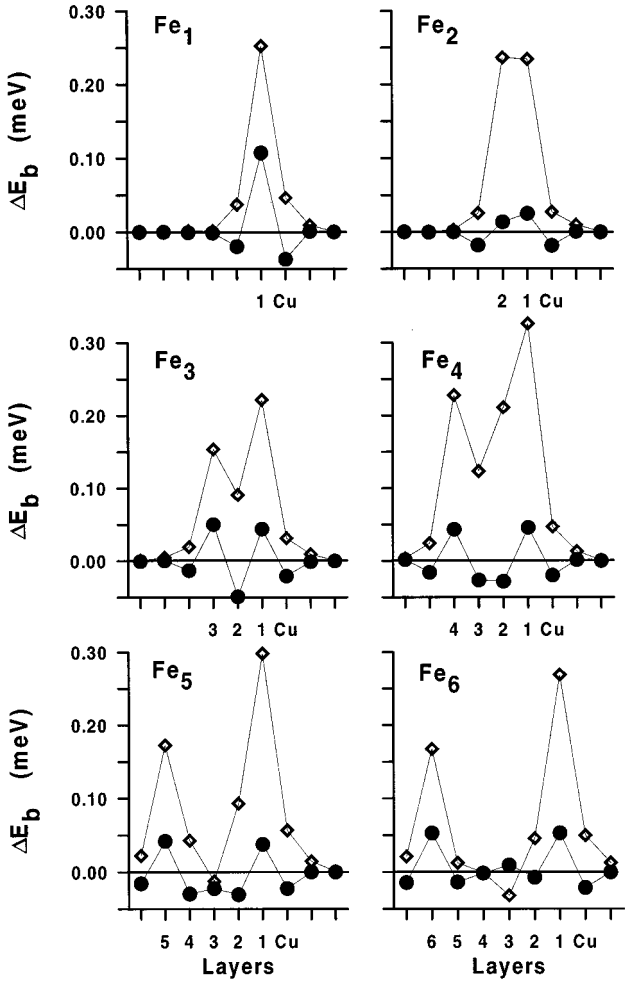

FIG. 3. Layer-resolved band energy contributions to the MAE for Cu_1Fe_n/Cu(001) multilayers. The position of the cap layer is labeled by ''Cu.'' Only the Fe layers are numbered. The contributions related to the minority and majority channels (see text) are shown as open squares and solid circles, respectively. Solid lines serve as a guide for the eye.

From Figs. 2, 3, and 4 it is clear that the MAE is governed by contributions of the Fe layers, whereas only a small part of the MAE comes from the substrate layer closest to the Fe film or from the capping Cu layers. Moreover, in these regions the majority and minority contributions almost cancel

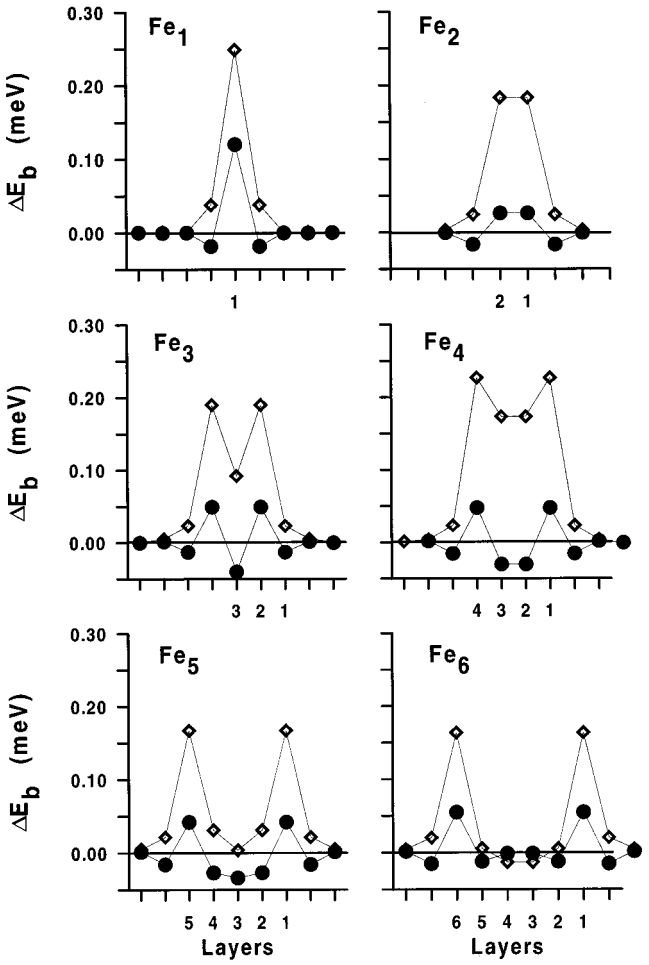

FIG. 4. Layer-resolved band energy contributions to the MAE for $Cu_\infty Fe_n/Cu(001)$ multilayers. Only the Fe layers are numbered. The contributions related to the minority and majority channels (see text) are shown as open squares and solid circles, respectively. Solid lines serve as a guide for the eye.

each other. Note that in the case of a Au substrate much larger contributions of gold to the MAE were found,[22] which as compared to copper can be attributed to the larger spin-orbit splitting of gold. The asymmetry of the local charges and magnetic moments of the $Fe_n/Cu(001)$ overlayers shows up in Fig. 2 as a dominating feature in the layer-resolved $\Delta E_b^{\downarrow}$ contributions to the MAE. The largest contribution arises from Fe(n), whereas $\Delta E_b^{\downarrow}$ of Fe(1) is almost negligible. Especially for $2 \leqslant n \leqslant 5$, a systematic decrease in $\Delta E_b^{\downarrow}$ can be observed when going from the substrate to the surface. It should be noted that a qualitatively similar behavior of the layer-resolved ΔE_b has been found also for $Fe_n/Au(001)$.[22]

Consequently, by introducing a new interface of Fe and Cu, i.e., by putting a cap of Cu layer(s) onto the Fe film, the MAE generally increases. This is clearly seen in Fig. 3, namely, for the case of a cap of one Cu layer ($m=1$). With reference to the uncapped case, $\Delta E_b^{\downarrow}$ is dramatically enhanced for the Fe monolayer and for Fe(1) in multilayers ($n \geqslant 2$). A remarkable feature of this figure is also that for $n>2$ $\Delta E_b^{\downarrow}$ of Fe(1) is systematically larger than that of Fe(n).

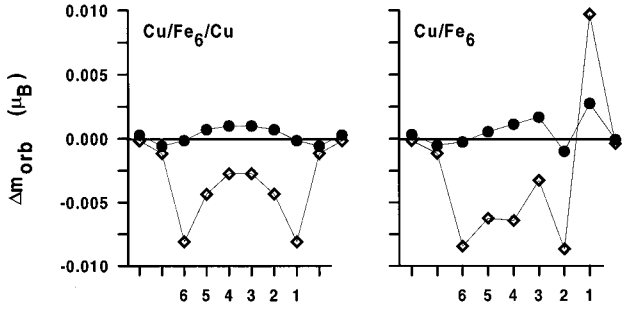

FIG. 5. Layer-resolved orbital anisotropies $\Delta m_{\mathrm{orb}} = m_{\mathrm{orb}}^{\parallel} - m_{\mathrm{orb}}^{\perp}$ for $Cu_\infty/Fe_6/Cu(001)$ (Cu/Fe_6/Cu) and $Fe_6/Cu(001)$ (Cu/Fe_6) multilayers, as decomposed into majority (solid circles) and minority (open squares) components. Only the Fe layers are labeled. Solid lines serve as a guide for the eye.

Another characteristic feature of Fig. 1 is the anomalous peak of ΔE_b at $n=4$ for the capped multilayers. This point can be enlightened in terms of the layer resolved ΔE_b's for the interlayer systems, i.e., for the case of $m=\infty$. From Fig. 4 one can see that for $n=5$ and especially for $n=6$ the buried Fe layers contribute very little to ΔE_b. We have checked but not shown in Fig. 4 that this is valid also for $n=7$ and 8. Therefore, for $n \geqslant 6$, ΔE_b arises exclusively from the vicinity of the two interfaces and, consequently, becomes constant with increasing film thickness. For $n \leqslant 4$, however, all the Fe layers have considerable contributions to $\Delta E_b^{\downarrow}$, which, as can be seen in Fig. 1, give rise to a monotonous increase of ΔE_b up to $n=4$.

Comparing the entries for $n=6$ in Figs. 2 and 4, it is quite surprising that the buried Fe layers contribute very differently to ΔE_b: While for $m=0$ their contribution is non-negligible, for $m=\infty$ practically no contribution arises from this region of the film. This, however, explains why, for $n=5$ and 6, ΔE_b becomes smaller in the case of $m=\infty$ than for $m=0$ (see Fig. 1). Since, as can be seen from Tables I, II, and III, the corresponding layers hardly differ in terms of local quantities, the above feature of $\Delta E_b^{\downarrow}$ indicates an unexpected dependence of the magnetocrystalline anisotropy on the ''boundary conditions.'' For thicker films of Fe sandwiched by bulk Cu a basically localized interface anisotropy is built up, while for a free surface of the Fe multilayers on Cu(001) the anisotropy seems to extend over the whole film. Such a kind of spatially extended magnetocrystalline anisotropy has already been reported even for thick Fe, Co, and Ni slabs by Cinal *et al.*[31]

D. Orbital moment anisotropy

For the above two particular cases, namely, for $Cu_\infty Fe_6/Cu(001)$, and $Fe_6/Cu(001)$, also the anisotropy of the orbital moments is characteristically different. In Fig. 5 the layer-resolved orbital anisotropies as decomposed again into majority and minority spin contributions are shown for $m=0$ and $m=\infty$. According to perturbation theory,[26,27] the magnetic anisotropy is generally accompanied by an enhancement of the orbital moment along the preferred direction. As compared to the corresponding entries in Figs. 2 and 4, especially for the interlayer case the minority contribu-

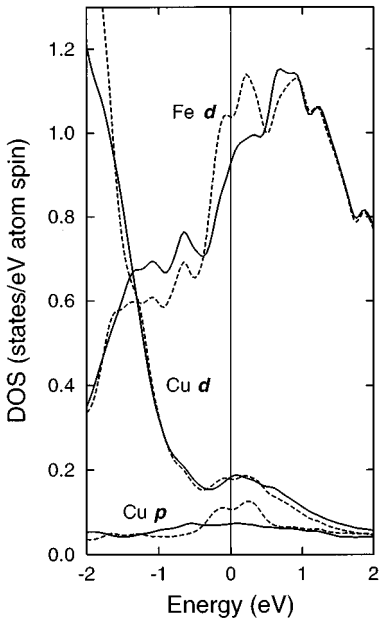

FIG. 6. Layer-resolved partial minority densities of states in the vicinity of the Fermi level (zero of the energy scale) for a $Cu_1/Fe_6/Cu(001)$ multilayer. Solid lines, Fe(6) and the topmost substrate Cu layer; dashed lines, Fe(1) and the Cu cap.

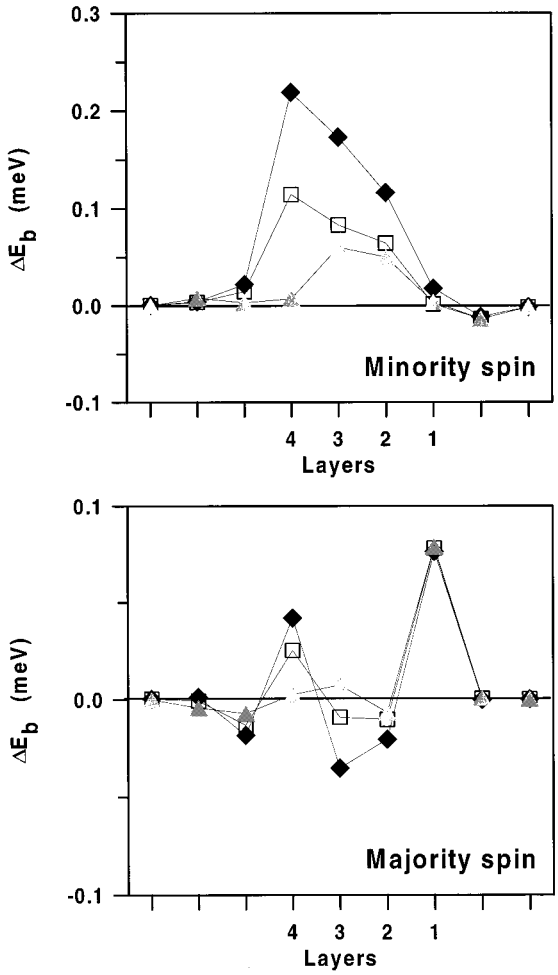

FIG. 7. Layer-resolved band energy contributions to the MAE for $Fe_4/Cu(001)$ multilayers interdiffused at the Fe/Cu interface: diamonds, 0%; squares, 15%; triangles, 30%. Only the Fe layers are numbered. For the interface layer of the Fe film (numbered by 4) only the contribution of the Fe component is displayed, whereas for the interface layer of the substrate (one layer to the left) only the contribution of the Cu component is displayed.

tions of the band energy anisotropy and the orbital moment anisotropy display a remarkably similar shape with respect to the layers. A linear proportionality, however, does not apply, since, e.g., $\Delta E_b^{\downarrow}$ changes sign in the middle of the film while the orbital moment anisotropy does not. An obviously different behavior can be seen for the free surface case, where for Fe(1) a definite increase of the orbital moment with respect to the in-plane direction is found, whereas $\Delta E_b^{\downarrow}$ of Fe(1) is positive; i.e., it supports a perpendicular direction of the magnetization. This observed peculiarity of the orbital moment anisotropy indicates that the simple qualitative predictions of perturbation theory do not in general apply for multilayers: Only for systems with localized anisotropy contributions such as for thick interlayers is roughly the expected relationship between the layer resolved orbital moment anisotropies and MAE's found, whereas for systems with a spatially extended anisotropy a corresponding relationship can hardly be established.

E. Role of interfacial hybridization

The basic characteristics of the MAE's as discussed before can also be viewed by adopting the arguments of Zhong *et al.*,[32] who very recently investigated the magnetocrystalline anisotropy of a Co monolayer on Cu(111) capped by further Cu layers and who concluded that interfacial hybridization has a dominant effect on the MAE. In Ref. 32 the key role is attributed to the energy separation between the *d* band of Co and that of the subsequent cap layer. In order to check the validity of this idea for the present system, for the special case of $Cu_1Fe_6/Cu(001)$ the minority *d*-like density of states (DOS) of Fe(1) and Fe(6) is shown in the vicinity of the Fermi level together with the *p*- and *d*-like DOS's of the topmost substrate Cu layer and the capping Cu layer (see Fig. 6). Apparently, due to increased hybridization with mainly Cu *p* states, some Fe states of minority *d*-like character, which for Fe(6) lie below the Fermi level, are shifted upwards for Fe(1). Indeed, due to the enhanced surface potential, the bands of the cap layer move energetically closer to the minority *d* band of Fe(1) as compared to the corresponding bands at the interface with the substrate, leading thus to a different hybridization. By using a symmetry-adapted basis corresponding to the underlying C_{4v} point group, it turned out that the hybridized states seen in Fig. 6 mainly belong to the Δ_5 irreducible representation, which comprises p_x, p_y, d_{xz}, and d_{yz} orbitals ($\ell \leq 2$). As indicated also by second-order perturbation theory,[26,27] an increased weight of d_{xz} and d_{yz} states around the Fermi level gives rise to an enhancement of the MAE.[32]

This kind of surface effect obviously vanishes for multilayers capped by more than one Cu layer, because in that case the Cu layer neighboring the topmost Fe layer does not lie directly at the surface. This immediately explains why the MAE generally reduces for these systems as compared to

multilayers capped by only one Cu layer. Hybridization also offers a possible interpretation of the anomalous peak at $n=4$ for capped multilayers, since up to $n=4$ interfacial hybridization seems to increase by the presence of both interfaces and to comprise also buried Fe layers, while for thicker films it has to decrease and to become spatially located in the vicinity of the interfaces.

It is commonly believed that formations of hybridized states as discussed above are particularly important for an understanding of the material specific features of the surface magnetic anisotropy, leading to the famous ''anomalous perpendicular anisotropy'' in several systems as investigated experimentally[33–36] and also studied recently by first principles calculations.[32,37] It should also be noted that since surface relaxation directly influences the hybridization between the magnetic film and the metallic cap, an inclusion of surface relaxation possibly modulates the calculated MAE's.[32]

F. Effect of interdiffusion

As an additional factor that can modulate the MAE, we also investigated the effect of interdiffusion at the interface of Cu and Fe. For the particular case of Fe_4/Cu(001) we carried out calculations allowing intermixing at the interface in terms of the coherent-potential approximation for random (surface) alloys in a similar way as was recently used, e.g., by Turek *et al.*[38] In the present case, therefore, the ''top substrate'' and the subsequent ''film layer'' were formed by layers of $Cu_{1-c}Fe_c$ and $Fe_{1-c}Cu_c$, respectively, while all the other layers remained compositionally unchanged. In Fig. 7 the layer-resolved $\Delta E_b^{\uparrow}$'s and $\Delta E_b^{\downarrow}$'s are shown for $c=0$, 0.15, and 0.30. As expected, dramatic changes occur at the interface Fe layer; namely, at 30% intermixing both the minority and majority contributions of Fe vanish. Although the subsequent two Fe layers are compositionally not affected by the intermixing, the band energy anisotropy is remarkably reduced also in these layers. Since a realistic inclusion of intermixing effects would require realistic concentration profiles possibly deduced from experiments, for systems that exhibit considerable interdiffusion a quantitative comparison of theoretical data to experiments is expected to be very difficult.

IV. CONCLUDING REMARKS

Experimentally the physical properties of Fe_n/Cu(001) samples are classified by the growth conditions, especially by the growth temperature.[2,10] It is tempting to associate samples grown at room temperature with the antiferromagnetic phase and low-temperature samples with the ferromagnetic one. With respect to the ferromagnetic phase, there seems to be a controversy between the experimental measurements and our calculations for the free surface case, since experimentally there is an orientational transition from the perpendicular to an in-plane orientation of the magnetization at about five to six monolayers of Fe, while our calculations always predict an in-plane arrangement. It was pointed out by Giergel *et al.*,[2] however, that the uncovered low-temperature samples are of poor quality, and the perpendicular orientation is due to reasons other than the electronic structure. It should be mentioned also that for higher growth temperatures diffusion of a Cu layer onto the surface was observed experimentally.[1] This not only improves the film quality,[39] but according to our calculations also induces a switching from a perpendicular to in-plane orientation of magnetization at about five Fe layers.

ACKNOWLEDGMENTS

Enlightening discussions with B.L. Györffy, R. Monnier, and J. Kirschner are kindly acknowledged. We thank A.J. Freeman and Lieping Zhong for sending us their manuscript prior to publication. The research presented in this paper was supported by the Austrian Ministry of Science (Grant Nos. GZ. 45.368/2-IV/6/94 and GZ. 308.941/2-IV/3/95), by the Austrian National Bank (P4648), and by the Hungarian National Scientific Research Foundation (Grant Nos. OTKA F014378 and OTKA 016740).

[1] Th. Detzel and N. Memmel, Phys. Rev. B **49**, 5599 (1994).
[2] J. Giergiel, J. Shen, J. Woltersdorf, A. Kirilyuk, and J. Kirschner, Phys. Rev. B **52**, 8528 (1995).
[3] R. Allenspach, J. Magn. Magn. Mater. **129**, 160 (1994).
[4] R. Allenspach and A. Bischof, Phys. Rev. Lett. **69**, 3385 (1992).
[5] S. F. Cheng, A. N. Mansour, J. P. Teter, K. B. Hathaway, and L. T. Kabacoff, Phys. Rev. B **47**, 206 (1993).
[6] D. Pescia, M. Stampanoni, G. L. Bone, A. Vateriaus, R. F. Willis, and F. Meier, Phys. Rev. Lett. **58**, 2126 (1987).
[7] M. Stampanoni, A. Vateriaus, M. Aeschliman, F. Meier, and D. Pescia, J. Appl. Phys. **64**, 5321 (1988).
[8] Th. Detzel, M. Vonbank, M. Donath, and V. Dose, J. Magn. Magn. Mater. **147**, L1 (1995).
[9] F. Baudelet, Phys. Rev. B **51**, 12 563 (1995).
[10] Dongqi Li, M. Freitag, J. Pearson, Z. Q. Qiu, and S. D. Bader, J. Appl. Phys. **76**, 6425 (1994).
[11] J. Thomassen, F. May, B. Feldman, M. Wuttig, and H. Ibach, Phys. Rev. B **48**, 10 284 (1993).
[12] G.J. Mankey, R.F. Willis, and F.J. Himpsel, Phys. Rev. B **48**, 10 284 (1993).
[13] C.L. Fu and A.J. Freeman, Phys. Rev. B **35**, 925 (1987).
[14] T. Kraft, P.M. Marcus, and M. Scheffler, Phys. Rev. B **49**, 11 511 (1994).
[15] M. Doyama, M. Matsui, H. Matsuoka, S. Mitani, and K. Doi, J. Magn. Magn. Mater. **93**, 374 (1991).
[16] S. Mitani, A. Kida, and M. Matsui, J. Magn. Magn. Mater. **126**, 76 (1993).
[17] M. Aldén, S. Mirbt, H.L. Skriver, N.M. Rosengaard, and B. Johansson Phys. Rev. B **46**, 6303 (1992) and references therein.
[18] G.Y. Guo, W.M. Temmerman, and H. Ebert, J. Phys. Condens. Matter **3**, 8205 (1991).
[19] G.Y. Guo, W.M. Temmerman, and H. Ebert, J. Magn. Magn. Mater. **104–107**, 1772 (1992).
[20] L. Szunyogh, B. Újfalussy, P. Weinberger, and J. Kollár, Phys. Rev. B **49**, 2721 (1994).
[21] R. Zeller, P.H. Dederichs, B. Újfalussy, L. Szunyogh, and P.

Weinberger, Phys. Rev. B **52**, 8807 (1995).
[22] L. Szunyogh, B. Újfalussy, and P. Weinberger, Phys. Rev. B **51**, 9552 (1995).
[23] S.H. Vosko, L. Wilk, and M. Nusair, Can. J. Phys. **58**, 1200 (1980).
[24] U. von Barth and L. Hedin, J. Phys. C **5**, 1629 (1972).
[25] R. Lorenz and J. Hafner, J. Phys. Condens. Matter **7**, L253 (1995).
[26] P. Bruno, Phys. Rev. B **39**, 865 (1989).
[27] P. Bruno (unpublished).
[28] J.B. Staunton, B.L. Györffy, J. Poulter, and P. Strange, J. Phys. C **21**, 1595 (1988).
[29] J.B. Staunton, M. Matsumoto, and P. Strange, in *Application of Multiple Scattering Theory to Materials Science*, edited by W. H. Butler *et al.*, MRS Symposia Proceedings No. 253 (Materials Research Society, Pittsburgh, 1992), p. 309.
[30] B. Újfalussy, L. Szunyogh, and P. Weinberger, Phys. Rev. B **51**, 12 836 (1995).
[31] M. Cinal, D.M. Edwards, and J. Mathon, Phys. Rev. B **50**, 3754 (1994).
[32] Lieping Zhong, Miyoung Kim, Xindong Wang, and A.J. Freeman, Phys. Rev. B **53**, 9770 (1996).
[33] B.N. Engel, M.H. Wiedmann, R.A. Van Leeuwen, and C.M. Falco, J. Appl. Phys. **73**, 6192 (1993); B.N. Engel, M.H. Wiedmann, and C.M. Falco, Phys. Rev. B **48**, 9894 (1993); B.N. Engel, M.H. Wiedmann, and C.M. Falco, J. Appl. Phys. **75**, 6401 (1994).
[34] P. Beauvillain, A. Bobouh, C. Chappert, S. Ould-Mahfoud, J.P. Renard, P. Veillet, D. Weller, and J. Corno, J. Appl. Phys. **76**, 6078 (1994).
[35] J. Kohlhepp and U. Gradmann, J. Magn. Magn. Mater **139**, 347 (1995).
[36] M.E. Buckley, F.O. Schumann, and J.A.C. Bland, Phys. Rev. B **52**, 6596 (1995).
[37] B. Újfalussy, L. Szunyogh, P. Bruno, and P. Weinberger, Phys. Rev. Lett. **77**, 1805 (1996).
[38] I. Turek, J. Kudrnovský, V. Drchal, M. Šob, and P. Weinberger, Phys. Rev. Lett. **74**, 2551 (1994).
[39] H. Magnan, D. Chandesris, B. Vilette, O. Heckmann, and J. Lecante, Phys. Rev. Lett. **67**, 859 (1991).